Photoacoustic and ESR studies of iron-doped soda-lime glasses: Thermal diffusivity

A. M. Mansanares, M. L. Baesso, E. C. da Silva, F. C. G. Gandra, and H. Vargas
Instituto de Física, Universidade Estadual de Campinas, Caixa Postal 6165, 13081 Campinas, São Paolo, Brazil

L. C. M. Miranda
Laboratório Associado de Sensores e Materiais, Instituto de Pesquisas Espaciais, Caixa Postal 515, 12201 S.J. Campos, São Paolo, Brazil

(Received 8 May 1989)

The photoacoustic technique is used to measure the thermal diffusivity of iron-doped soda-lime glasses. To explain the thermal diffusivity behavior as a function of the iron content in the samples, electron-spin-resonance data were used. It is concluded that the main reason for the observed changes in the thermal diffusivity is the ferric ion entering substitutionally at the Si^{4+} sites.

I. INTRODUCTION

The photoacoustic (PA) technique has been proved over the last ten years to be a valuable technique for measuring the thermal diffusivity α of solid samples. For a review on the subject we refer to Refs. 1–3. The importance of the thermal diffusivity as a physical parameter to be monitored is based on the fact that it is unique for each material. This can be appreciated by the tabulated values of α presented by Touloukian *et al.*[4] The PA measurement of the thermal diffusivity has been carried out using different techniques.[5–10] In particular, in the case of glasses the PA technique has been applied to the investigation of the influence of dopants on both the thermal diffusivity[11,12] and the optical-absorption spectrum.[13,14]

In this paper we report on the role of ferric ions in the changes of the thermal diffusivity of soda-lime glasses. The thermal diffusivity was measured using the PA phase-lag method as reported in Ref. 11. To understand the observed changes of the thermal diffusivity as a function of the iron concentration we have also studied the electron-spin-resonance (ESR) spectra of our samples. In this way we could assign the atomic surroundings of iron in the glass matrix and correlate them to the observed changes in the thermal diffusivity. We concluded that the main reason for the observed changes of the doped-glass thermal diffusivity are the ferric ions substituting silicon in the glass structure.

II. EXPERIMENTAL

The soda-lime glass samples were prepared from standard-grade chemicals. The basic composition was identical and equal to 72 wt. % SiO_2, 18 wt. % Na_2O, and 10 wt. % CaO. The doped samples were prepared by melting the basic glass with varying concentrations (wt. %) of Fe_2O_3. The samples were melted in a platinum crucible in an electric furnace at 900 °C followed by an intermediate annealing at 525 °C.

The PA measurements were carried out using the two-beam experimental arrangement as described in Refs. 9 and 11. The light from a 120-W tungsten lamp, after being chopped, is divided by a beam splitter and the resulting beams are directed to opposite sides of the PA cell as shown in Fig. 1. The PA cell is a conventional brass cell in which a quarter-inch condenser microphone (Bruel & Kjaer) is mounted in one of its walls. The samples, in the shape of 8-mm-diam disks, were flush against the back wall of the cell, which has a 4-mm-diam hole through which the rear beam passes. According to Refs. 9, 11, and 12 the thermal diffusivity, for an optically opaque sample, is obtained by measuring the relative phase lag $\Delta\phi=\phi_F-\phi_R$, at a single modulation frequency, between the rear surface illumination (R) and the front (F) surface illuminations. This phase lag obeys the equation

$$\tan(\Delta\phi)=\tanh(la)\tan(la)\ , \tag{1}$$

where l is the sample thicknesses, $a=(\pi f/\alpha)^{1/2}$ is the sample thermal diffusion coefficient, f is the modulation frequency, and α is the sample thermal diffusivity. It follows from Eq. (1) that the procedure to determine α is to substitute the experimental value of $\Delta\phi$ into Eq. (1) and solve it for $z=la$. Knowing z, the thermal diffusivity is readily given by $\alpha=\pi f l^2/z^2$. The above method requires, however, the sample to be optically opaque. To ensure the optical opaqueness condition a thin circular Al

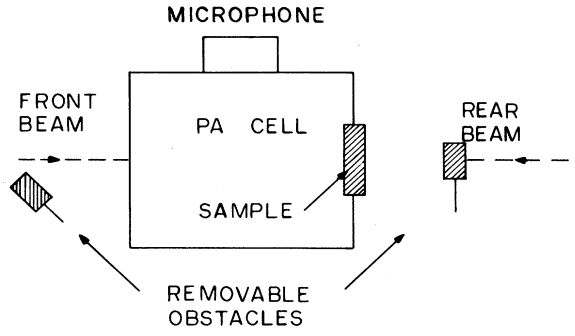

FIG. 1. Experimental arrangement for the two-beam photoacoustic measurement of the thermal diffusivity.

foil 20 μm thick and 2 mm in diameter was attached to each side of the samples using a thin layer of diffusion pump oil.

The ESR measurements were performed on a Varian E-12 spectrometer operating at the X band at room temperature. The ESR data were determined from the fittings of the experimental data to the first derivative of a Lorentzian curve. The intensity of the ESR signal was assumed to be proportional to the product of the peak-to-peak height and the square of the linewidth.

III. RESULTS AND DISCUSSION

In Fig. 2 we show the dependence of α on the Fe_2O_3 concentration. This plot shows that starting from $\alpha=0.0046$ cm^2/s, the thermal diffusivity exhibits a saturation around $\alpha=0.0054$ cm^2/s for doping concentrations above roughly 4%. To understand the mechanism responsible for this saturation we have carried the ESR measurements of the ferric ions. In Fig. 3 we show the ESR spectra for two samples having doping concentrations of (a) 1% and (b) 8%. For the 1% Fe_2O_3-doped sample, the ESR spectrum exhibits resonances at $g=1.9$, 4.3, and 7.6. As the Fe_2O_3 concentration is increased to 8% the resonance at $g=2.0$ gets greatly enhanced. The above spectra are similar to the ones previously reported in the literature[15–20] for Fe^{3+} ions in borate and silicate glasses. The ESR of Fe^{3+} in glasses is discussed in terms of the possible atomic surroundings it can have. The ferric ion can occupy basically three different sites. It can be a network former, occupying sites similar to a silicon ion. In this case it is tetrahedrally surrounded by oxygen ions. It can also be in a network-modifying position, in which case it occupies the interstices of the glass structure rather than the center of an oxygen tetrahedron. Finally Fe^{3+} can be positioned in aggregates such as Fe_2O_3 due to the excess oxide which did not interact with the glass structure. Hereafter, we denote these three sites as sites A, B, and C, respectively. In site C, the g value is that of the free ion, namely, $g=2.0$, since it is due to Fe^{3+} in the oxide. In an interstitial position (i.e., site B), the ferric ion is expected to exhibit also a broad resonance around $g=2.0$, as discussed by Castner *et al.*[25] In other words, sites B and C give rise to isotropic superimposed broad lines at $g=2.0$. For samples with 4% and 8% Fe_2O_3, the linewidths of the $g=2.0$ lines, due to sites B and C, vary from 300 to 400 G and from 900 to 1100 G, respectively. Site A, in contrast, is responsible for the large g resonances. For a detailed discussion on the large resonances of Fe^{3+} in glasses we refer to Refs. 15 and 18. Castner *et al.*[15] have explained the large g resonances as being due to the presence of terms in the fine-structure part of the spin Hamiltonian representing low-symmetry distortions due to the local electric field. The ground state of the free ferric ion is ^6S and so the high-spin ferric ion has $S=\frac{5}{2}$ and no first-order spin-orbit interaction. Thus, when there is a large splitting of the ground manifold it is reasonable to describe the crystal-field Hamiltonian H_0 as[15,18–20]

$$H_0=D[S_z^2-\tfrac{1}{3}S(S+1)]+E(S_x^2-S_y^2) \tag{2}$$

so that the complete Hamiltonian for the ESR experiment is

$$H=g\beta\mathbf{H}\cdot\mathbf{S}+H_0\ , \tag{3}$$

where the first term in Eq. (3) is the usual Zeeman term with β the Bohr magneton and H_0 given by Eq. (2). Rewriting the H_0 in units of E, $H_0=Eh_0$, and defining the parameter $\lambda=D/E$ we get

$$h_0=\lambda[S_z^2-\tfrac{1}{3}S(S+1)]+S_x^2-S_y^2\ . \tag{4}$$

Diagonalizing h_0 in the $S=\frac{5}{2}$ manifold we find three dou-

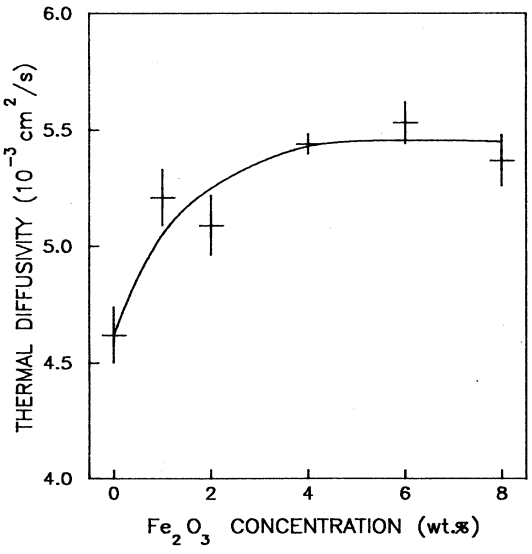

FIG. 2. Dependence of the thermal diffusivity, as obtained from the photoacoustic phase-lag method, as a function of the iron oxide doping concentration.

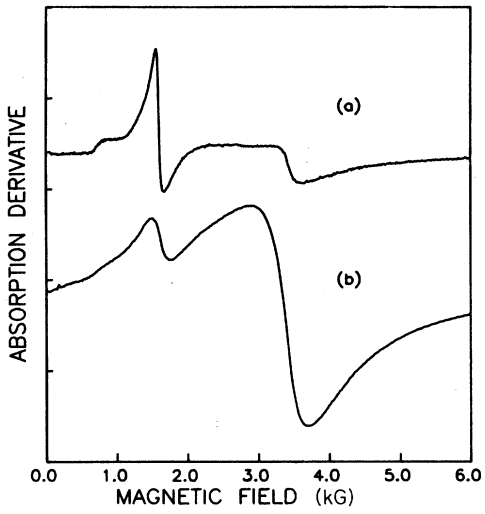

FIG. 3. ESR spectra recorded at room temperature and at 9.514 GHz for the glass samples having (a) 1% and (b) 8% iron oxide doping concentrations.

blets, whose eigenvalues are functions of λ. In Fig. 4 we show the variation with λ of the effective g factors for the three crystal-field doublets. The above calculations followed closely the one reported by Wickman *et al.*[18] Figure 4 shows that for $\lambda=1.3$ the upper doublet gives us the same resonances as the ones observed in Fig. 3, namely, at $g=1.9$, 4.3, and 7.6. Another possibility for explaining the $g=4.3$ line would be the λ near zero situation. In this case, it follows from Fig. 4 that these lines would be accompanied by two lines with g values close to unity (roughly, g equal to 0.6 and 0.8) and another one near $g=10$. We have tried to find these two lines close to unity by carrying out data storage of up to 100 experimental runs. Despite this we could not observe these lines.

Summarizing, we may say that the ESR spectra indicate that the Fe^{3+} ion occupies three different sites such that only site A contributes to the $g=7.6$ and 4.3 resonances, whereas the $g=2.0$ line receives the contribution of all three of these sites. We have next carried out numerically the deconvolution of the spectra to calculate the peak-to-peak heights and linewidths of each line. Knowing the peak-to-peak heights and linewidths we could then calculate the line intensities and consequently the number of Fe^{3+} ions at the three different sites. In Fig. 5 we show the variation of the line intensities as a function of the iron concentration. Due to the superposition of the $g=2$ lines from sites B and C with the $g=1.9$ line from site A, we have characterized site A only by the line at $g=4.3$. Furthermore, the $g=2.0$ lines from sites B and C become relevant only for Fe_2O_3 concentrations above 4%. Figure 5 tells us that after an initial rise, the substitutional iron ($g=4.3$) line intensity exhibits a saturation for Fe_2O_3 concentrations above 4%. In contrast, the $g=2.0$ line intensities of the interstitial (site B) and free (site C) Fe^{3+} ions always rise with increasing Fe_2O_3 concentration above 4%. In other words, at low oxide concentrations, the ferric ions enter the glass structure substitutionally. At these network-forming sites the Fe^{3+} ions should have a strong probability of attracting a single positive charge, probably Na^+, to make them equivalent to the Si^{4+} ions. The number of these substitutional Fe^{3+} ions saturates for oxide concentrations around 4%. On increasing the oxide concentration above 4%, the incorporated Fe^{3+} ions locate themselves at interstitial positions and at excess iron oxide aggregates not interacting with the glass structure. At the interstitial sites, the ferric ion plays the role of a charge balancer, necessary to stabilize the substitutional Fe^{3+} ions which may become unstable due to changes in the number of Na^+ charge balancers. However, the fact that, above 4% oxide concentration, the $g=2.0$ line intensity due to site C is much greater than the one due to site B indicates that, above 4%, the Fe^{3+} ions are preferably located at excess oxide aggregates.

Comparing the ESR line intensities' behavior as a function of the oxide concentration with that of the thermal diffusivity shown in Fig. 2, we conclude that the main responsibility for the observed changes of the thermal diffusivity with the iron doping may be ascribed to the Fe^{3+} ions entering the network-forming sites. Figures 2 and 5 show that the $g=4.3$ line intensity and the thermal

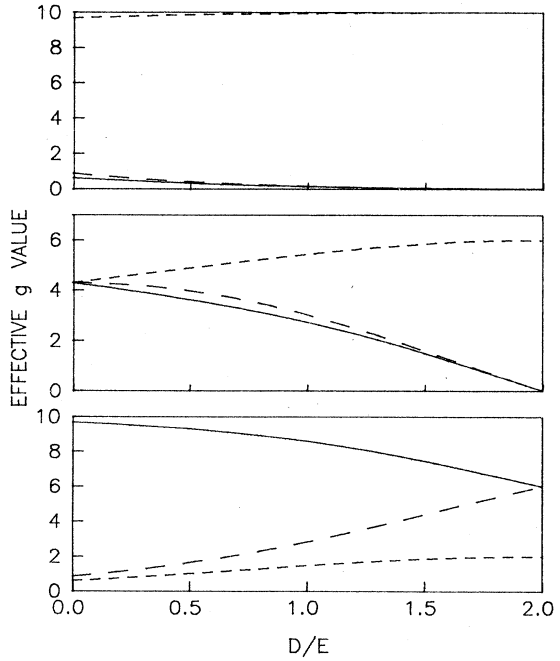

FIG. 4. Effective g values for the three crystal-field doublets for the spin Hamiltonian given by Eq. (4) of the text, as a function of the parameter λ.

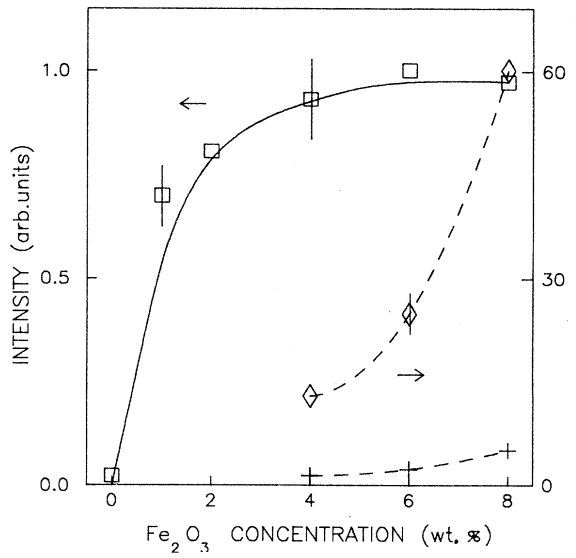

FIG. 5. Variation of the normalized line intensities for the $g=4.3$ (squares) line and the $g=2.00$ lines corresponding to site B (crosses) and site C (diamonds), as a function of the iron oxide doping concentration. The horizontal arrows indicate the scales to which the curves refer. The vertical lines at each experimental represent the corresponding error bars.

diffusivity curves not only exhibit the same behavior but also that on increasing the number of Fe^{3+} ions in sites B and C no further changes in α are observed. Furthermore, the excursions towards saturation for the $g=4.3$ line intensity and thermal diffusivity curves are within the same order of magnitude. The change in α to reach saturation corresponds to 15% of the saturation value, whereas the corresponding change of the $g=4.3$ line intensity is roughly 25% of the saturation value.

ACKNOWLEDGMENTS

This work was partially supported by Fundacão de Amparo e Pesquisa do Estado de São Paulo (São Paulo, São Paulo, Brazil), Conselho Nacional de Desenvolvimento Científico e Technológico (Rio de Janeiro, Rio de Janeiro, Brazil), and Coordenação de Aperfeiçoamento de Pessoal do Ensino Superior, Ministério da Educaçao e Cultura (Brazil).

[1]C. K. N. Patel and A. C. Tam, Rev. Mod. Phys. **53**, 517 (1981).
[2]J. B. Kinney and R. H. Stanley, Annu. Rev. Mater. Sci. **12**, 295 (1982).
[3]H. Vargas and L. C. M. Miranda, Phys. Rep. **161**, 43 (1988).
[4]L. R. Touloukian, R. W. Powell, C. Y. Ho, and M. C. Nicolaus, *Thermal Diffusivity* (Plenum, New York, 1973).
[5]M. J. Adams and G. F. Kirkbright, Analyst **102**, 678 (1977).
[6]R. T. Swimn, Appl. Phys. Lett. **42**, 955 (1983).
[7]C. L. Cesar, H. Vargas, J. Mendes Filho, and L. C. M. Miranda, Appl. Phys. Lett. **43**, 555 (1983).
[8]A. Lachaine and P. Poulet, Appl. Phys. Lett. **45**, 953 (1984).
[9]O. Pessoa, Jr., C. L. Cesar, N. A. Patel, H. Vargas, C. C. Ghizoni, and L. C. M. Miranda, J. Appl. Phys. **59**, 1316 (1986).
[10]L. F. Perondi and L. C. M. Miranda, J. Appl. Phys. **62**, 2955 (1987).
[11]A. C. Bento, H. Vargas, M. M. F. Aguiar, and L. C. M. Miranda, Phys. Chem. Glasses **28**, 127 (1987).
[12]M. L. Baesso, Z. P. Arguello, A. C. Bento, H. Vargas, and L. C. M. Miranda, in *Photoacoustic and Photothermal Phenomena,* edited by P. Hess and J. Pelzl (Springer, Heidelberg, 1988), p. 351.
[13]G. A. R. Lima, M. L. Baesso, Z. P. Arguello, E. C. da Silva, H. Vargas, and L. C. M. Miranda, Phys. Rev. B **36**, 9812 (1987).
[14]M. L. Baesso, A. M. Mansanares, E. C. da Silva, H. Vargas, and L. C. M. Miranda, Phys. Rev. B **40**, 1880 (1989).
[15]T. Castner, Jr., G. S. Newell, W. C. Holton, and C. P. Slichter, J. Chem. Phys. **32**, 668 (1960).
[16]D. Loveridge and S. Parke, Phys. Chem. Glasses **12**, 19 (1971).
[17]E. A. Harris, Phys. Chem. Glasses **28**, 196 (1987).
[18]H. H. Wickman, M. P. Klein, and D. A. Shirley, J. Chem. Phys. **42**, 2113 (1965).
[19]E. G. Deroname, M. Mestdagh, and L. Vielvoye, J. Catal. **33**, 169 (1974).
[20]A. N. Kotasthane, V. P. Shiralkar, S. G. Hedge, and S. B. Kulkarni, Zeolites **6**, 253 (1986).